International Journal of Nanomedicine

Dovepress
open access to scientific and medical research

Open Access Full Text Article

ORIGINAL RESEARCH

# Shape-dependent antimicrobial activities of silver nanoparticles

This article was published in the following Dove Press journal:
*International Journal of Nanomedicine*



Ja Young Cheon[1]
Su Jun Kim[1]
Young Ha Rhee[2]
Oh Hyeong Kwon[3]
Won Ho Park[1]

[1]Department of Advance Organic Materials and Textile System Engineering, Chungnam National University, Daejeon 34134, Korea; [2]Department of Microbiology and Molecular Biology, Chungnam National University, Daejeon 34134, Korea; [3]Department of Polymer Science and Engineering, Kumoh National Institute of Technology, Gumi 39177, Korea

**Purpose:** An important application of silver nanoparticles (Ag NPs) is their use as an antimicrobial and wound dressing material. The aim of this study is to investigate the morphological dependence on the antimicrobial activity and cellular response of Ag NPs.

**Materials and methods:** Ag NPs of various shapes were synthesized in an aqueous solution using a simple method. The morphology of the synthesized Ag NPs was observed via TEM imaging. The antimicrobial activity of the Ag NPs with different morphologies was evaluated against various microorganisms (*Escherichia coli* [*E. coli*], *Staphylococcus aureus* [*S. aureus*], *Pseudomonas aeruginosa* [*P. aeruginosa*]). The antimicrobial activity of the Ag NPs was also examined according to the concentration in terms of the growth rate of *E. coli*.

**Results:** The TEM images indicated that the Ag NPs with different morphologies (sphere, disk and triangular plate) had been successfully synthesized. The antimicrobial activity obtained from the inhibition zone was in the order of spherical Ag NPs > disk Ag NPs > triangular plate Ag NPs. In contrast, fibroblast cells grew well in all types of Ag NPs when the cell viability was evaluated via an MTT assay. An inductively coupled plasma mass assay showed that the difference in the antimicrobial activities of the Ag NPs was closely associated with the difference in the release rate of the Ag ions due to the difference in the surface area of the Ag NPs.

**Conclusion:** The morphological dependence of the antimicrobial activity of the Ag NPs can be explained by the difference in the Ag ion release depending on the shape. Therefore, it will be possible to control the antimicrobial activity by controlling the shape and size of the Ag NPs.

**Keywords:** silver nanoparticles, Ag NPs, different shape, antimicrobial activity, cell viability, ion release

## Introduction

Silver nanoparticles (Ag NPs) are used for many applications due to their various advantages including catalytic, optical, electrical and antimicrobial properties.[1,2] Ag NPs have received considerable attention for use as antimicrobial agents and have been shown to be effective for such use.[3–5] The antimicrobial mechanism of Ag NPs is generally considered to involve multiple-factors, targets and mechanisms.[6–8] The Ag NPs can adhere and interact with cell membranes and can damage the intracellular metabolic activity and permeability of the membrane, resulting in breakage of the cell morphology and intracellular content leakage.[8–10] The reactive oxygen species (ROS) generated by the Ag NPs and Ag ions released from the Ag NPs also damages the cell membrane and reacts with various functional proteins and DNA to interfere with the

Correspondence: Won Ho Park
Department of Advance Organic Materials and Textile System Engineering, Chungnam National University, Daejeon 34134, Korea
Tel +82 42 821 6613
Fax +82 42 823 3736
Email parkwh@cnu.ac.kr

submit your manuscript | www.dovepress.com
DovePress
http://doi.org/10.2147/IJN.S196472

metabolism and DNA synthesis. The damage of these various cells eventually leads to apoptosis.[8,11–14]

Since the antimicrobial mechanism of the Ag NPs is complex, the physical and chemical properties, including the size, shape and surface charge of the NPs, can have a great influence on their antimicrobial activity.[15–17] There are various studies on the synthesis of NPs with different sizes, shapes and coatings.[16–19] By comparing the antimicrobial activity of these various Ag NPs, the influence of the physical and chemical properties on the antimicrobial activity can be confirmed. For example, some studies reported that Ag for antimicrobial capability should be in ionic form of $Ag^+$ of Ag° cluster. The Ag NPs are advantageous in a faster release of Ag ions because of their high surface area. The first study on the antimicrobial properties of the Ag NPs with various forms was reported by Pal et al.[20] When comparing spherical, rod-shaped and truncated triangular Ag NPs, the truncated triangular Ag NPs showed the best antimicrobial activity. The difference in the antimicrobial activity could be interpreted from the viewpoint of surface area. In addition, the effect of various properties of the Ag and Au NPs on the antimicrobial activity is currently being investigated.[21–24]

In this study, three types of Ag NPs – sphere shape (Ag NSs), disk shape (Ag NDs) and triangular plate shape (Ag NTs) – were synthesized in an aqueous solution using simple method. The effect of the shape of the Ag NPs on the antimicrobial activity and cell viability was examined. The antimicrobial activity against *Escherichia coli* (*E. coli*), *Staphylococcus aureus* (*S. aureus*), *Pseudomonas aeruginosa* (*P. aeruginosa*) was evaluated using the paper disk method. Furthermore, the antimicrobial activity against *E. coli* was determined via optical density (OD) growth curve tests. On the other hand, the cell viability of the fibroblasts was also evaluated using 3-(4,5-dimethylthiazol-2yl)-2,5-diphenyl tetrazolium bromide (MTT) assay. To investigate the difference in the Ag ion release from the Ag NPs with different morphologies, the release rate of the Ag ion with times was analyzed via inductively coupled plasma (ICP) mass spectrometry.

# Materials and methods

## Materials

Various types of Ag NPs were synthesized in aqueous solution using a simple method. All materials for synthesis were soluble in water. Poly(vinyl pyrrolidone) (PVP, Mw 40,000) was purchased from Sigma Aldrich (St. Louis, MO, USA). Silver nitrate ($AgNO_3$) (purity 99.9%, Kojima Chemicals Co. Ltd., Sayama, Japan) and sodium borohydride ($NaBH_4$) (Samchun Chemicals, Pyeongteak, Korea) were used as Ag NP precursor and reducing agent, respectively. Hydrogen peroxide ($H_2O_2$) (30%, Junsei Chemicals Co. Ltd., Tokyo, Japan) and sodium citrate tribasic dihydrate ($Na_3CA$) (Sigma Aldrich) were used as an oxidant and a reducing agent to control the morphology of the Ag NPs.

## Synthesis of Ag NPs with different shapes

The Ag NPs were synthesized in three forms: Ag NSs, Ag NTs and Ag NDs. All samples were purged through argon (Ar) gas after the reaction. A detailed synthesis of the three types of Ag NPs is described in the sections below, and a simple schematic diagram of the Ag NP synthesis is shown in Figure 1.

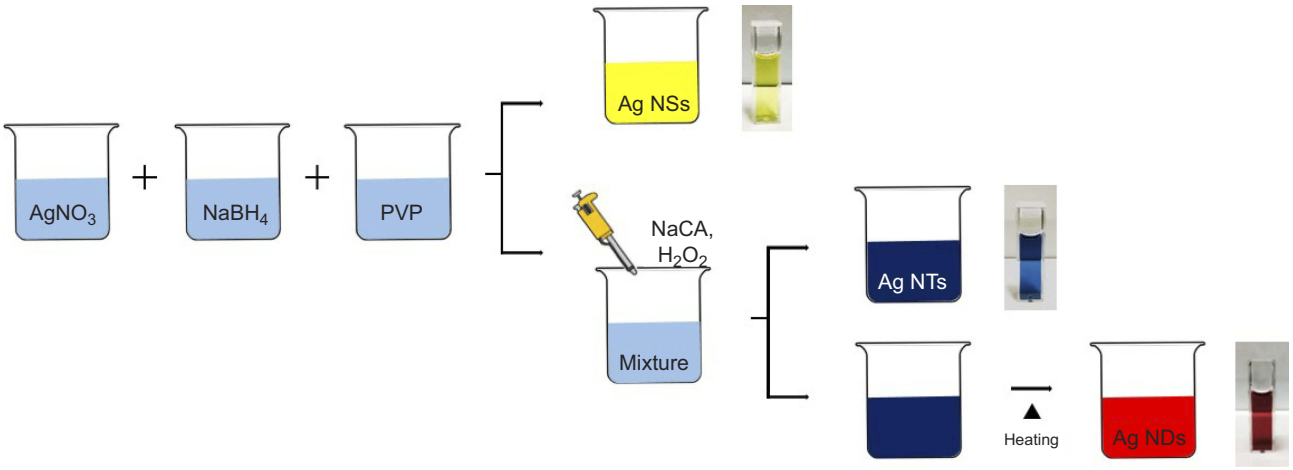


**Figure 1** Schematic illustration for synthesis of the Ag NPs with different shapes.
**Abbreviations:** Ag NPs, silver nanoparticles; $AgNO_3$, silver nitrate; Ag NDs, disk shape; Ag NSs, sphere shape; Ag NTs, triangular plate shape; $H_2O_2$, hydrogen peroxide; $NaBH_4$, sodium borohydride; PVP, poly(vinyl pyrrolidone).

### Preparation of the Ag NSs

Aqueous $AgNO_3$ solution (0.1 mM), aqueous PVP solution (0.7 mM) and aqueous $NaBH_4$ solution (100 mM) were prepared. Then, the Ag NSs were synthesized by mixing 25 mL of $AgNO_3$ solution, 1.5 mL of PVP solution and 0.14 mL of $NaBH_4$ solution. When all solutions were mixed, the solution color immediately changed from transparent to yellow. This confirmed the formation of the Ag NPs.

### Preparation of the Ag NTs

After mixing the three solutions in the same manner as the Ag NSs, $Na_3CA$ (1.5 ml, 30 mM) and $H_2O_2$ (90 µl) were added. As time passed, the solution color changed to blue through transparent, yellow, red, and violet.

### Preparation of the Ag NDs

After the $AgNO_3$ solution and $NaBH_4$ solution (100 mM) was mixed in the same concentration as the synthesis of the Ag NSs, PVP (0.06 g), $H_2O_2$ (240 µl) and $Na_3CA$ (1.8 mL, 100 mM) were added. After sufficient stirring, stirring stopped and the change in the solution color was observed. When the whole solution turned to blue, the Ag NDs was thermally synthesized in a water bath at 95°C.

## Antimicrobial activity test

The antimicrobial activity of the Ag NPs according to the morphology was confirmed by conducting the paper disk method and the OD growth curve test.

The paper disk test was incubated into a liquid medium after incubation for one day on an LB agar plate (*E. coli*), 30°C nutrient broth (NB) agar plate (*S. aureus, P. aeruginosa*) using a 37°C incubator. After obtaining a single colony using the loop, 50 mL medium was inoculated into shaking flasks (250 mL) for each strain. After incubation for 24 h with LB (37°C, 150 rpm) and NB (30°C, 150 rpm) in a shaking incubator, 1 mL was taken and sterilized in a 15 mL centrifuge tube. Serial dilutions of up to $10^{-3}$ were performed on 9 mL of the third distilled water. Then, 100 µL of each plate was plated on an LB agar plate (*E. coli*), NB agar plate (*P. aeruginosa, S. aureus*) according to the dilution ratio. After the paper disc was placed on the stained medium, 0.01 mg/mL of Ag NSs, Ag NDs, and Ag NTs were injected into the paper disc.

After incubation for 1 day in an LB agar plate (*E. coli*, 37°C), NB agar plate (*P. aeruginosa, S. aureus*, 30°C), the inhibition zone was observed. The antimicrobial activity of the Ag NPs (0 mg/mL, 0.1 mg/mL, 0.3 mg/mL, 0.5 mg/mL and 0.7 mg/mL) was measured on the basis of a 50-mL culture. After incubation in an LB agar plate (*E. coli*) for 1 day, the colonies were dissolved in 20-mL sterilized distilled water and seeded at 4% of the total volume at optical density 1.0–1.1. After that, the growth of *E. coli* was measured at 600 nm ($OD_{600}$) using a UV-Vis spectrometer at various concentrations.

## Cell viability assay

The cell viability of the synthesized Ag NSs, Ag NTs and Ag NDs was confirmed using fibroblast cells (NIH/3T3), which were purchased from Korean Cell Line Bank (Korea). The cell culture medium was Dulbecco's modified Eagle's medium (DMEM, WelGENE Inc., Korea) containing 10% fetal calf serum (FBS, WelGENE Inc., Korea) and 1% penicillin G-streptomycin (WelGENE Inc., Korea). And the cells were cultured in 96-well plates for 3 days and were tested at $2\times10^5$ cells/mL, and the cell growth was observed for 1, 3, 5 and 7 days. At this time, the concentration of the Ag NP added to each medium was set to 1 µg/mL, and the cell viability was evaluated using an MTT assay. There were also blank controls. Assays were read using an enzyme-linked immunosorbent assay (ELISA) reader.

## Characterizations

The color of the synthesized Ag NPs with different shapes was confirmed using photographs and SPR spectra due to the optical properties of the Ag NPs determined using a UV-VIS-NIR spectrophotometer (US 8453, Agilent Technologies, CA, USA). The zeta-potential and dynamic light scattering (DLS) data of the Ag NPs were obtained using a Zeta sizer ZS90 (Malvern, Worcestershire, UK). For the transmission electron microscopy (TEM) (Tecnai G2 F30, FEI Company, OR, USA), the samples were prepared by dropping the solution containing Ag NPs onto the carbon-coated copper grid. The average diameter of the Ag NPs with various shapes was obtained by analyzing the TEM images using a custom-code Scope Eye II image analysis program (Masan, Korea). Energy-dispersive X-ray (EDS) analysis data were taken using a TEM coupled with an EDS analysis attachment. The Ag ion release behavior of the Ag NPs with different morphologies was confirmed using an inductively coupled plasma (ICP) mass spectrometer (ELAN DRC II, Perkin-Elmer, MA, USA) with time.

## Results and discussion

### Characterization of the Ag NPs with different shapes

Various types of Ag NPs were analyzed using UV-VIS-NIR spectrometry. In Figure 2, the Ag NSs, Ag NTs and Ag NDs showed yellow, blue and red color, respectively, and the maximum absorption peaks corresponding to surface plasmon resonance (SPR) were observed at 410, 820 and 510 nm, respectively. For the Ag NTs and Ag NDs, a weak shoulder around 330 nm was also attributed to the out-of-plane quadruple resonance of the Ag nanoplate.[25]

The zeta-potentials of the Ag NSs, Ag NTs and Ag NDs measured using Zeta sizer were −13.8 mV, −28.6 mV and −29.2 mV, respectively. And the average sizes of the Ag NSs, Ag NTs and Ag NDs in aqueous solution were 38.5 nm, 51.1 nm and 50.6 nm, respectively. The morphology of the Ag NPs was confirmed via TEM imaging (Figure 3A). All three types of Ag NPs were observed in a well-dispersed form, each of which was a sphere, disc and triangular plate. Both the sphere and disc were circular, but the disc was a plate with lower density than the sphere, so it looks a little lighter in color. In addition, the discs and triangular plates were stacked vertically on the TEM grid (data not shown). In Figure 3B, all three types of Ag NSs, Ag NDs and Ag NTs showed the peak of Ag (3.0 KeV) in the elemental analysis obtained via EDS.[26]

### Antimicrobial activity of Ag NPs with different shapes

The antimicrobial properties of the Ag NPs were examined using *E. coli, S. aureus* and *P. aeruginosa*. The inhibition zone was evaluated using the disk diffusion method for all Ag NPs (Ag NSs, Ag NDs and Ag NTs) against *E. coli* (Figure 4A). Among these, the Ag NSs showed the widest

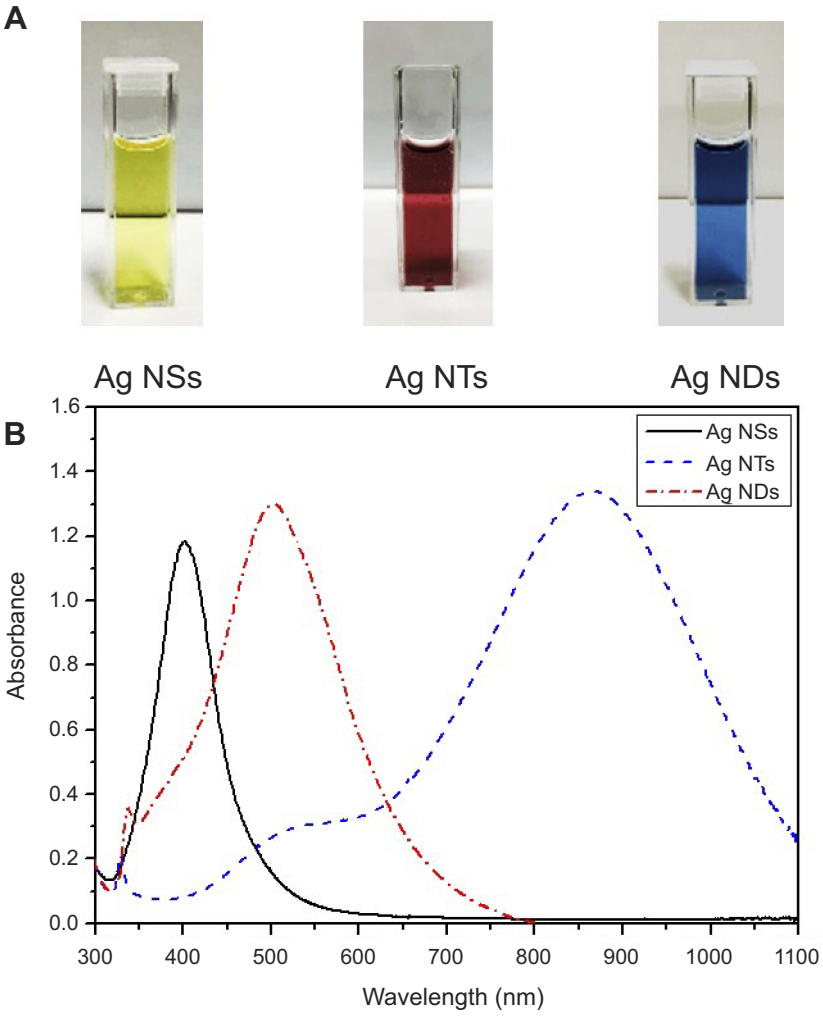


**Figure 2** (**A**) Solution color and (**B**) UV-VIR-NIR spectra of Ag NPs with different shapes.
**Abbreviations:** Ag NPs, silver nanoparticles; Ag NDs, disk shape; Ag NSs, sphere shape; Ag NTs, triangular plate shape.

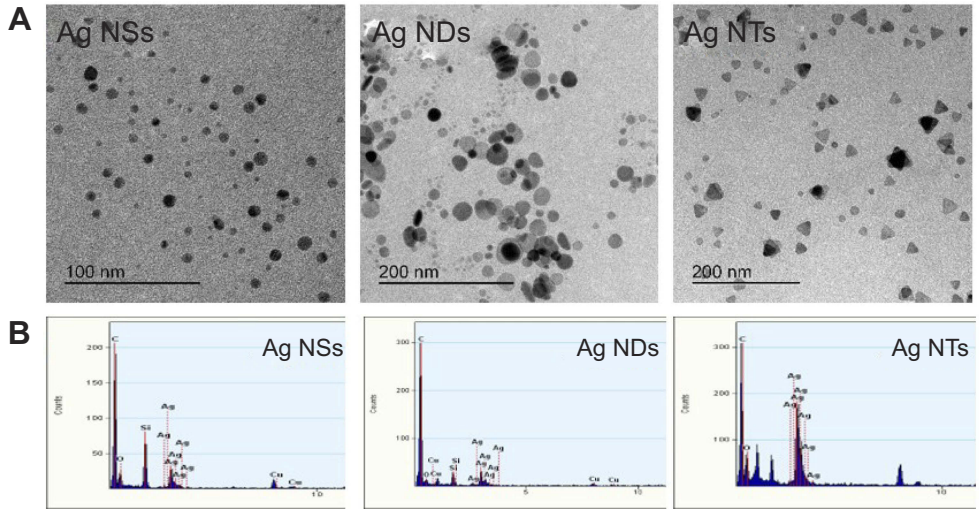


**Figure 3** (**A**) TEM images and (**B**) EDS spectra of Ag NPs with different shapes.
**Abbreviations:** Ag NPs, silver nanoparticles; Ag NDs, disk shape; Ag NSs, sphere shape; Ag NTs, triangular plate shape; EDS, energy-dispersive X-ray.

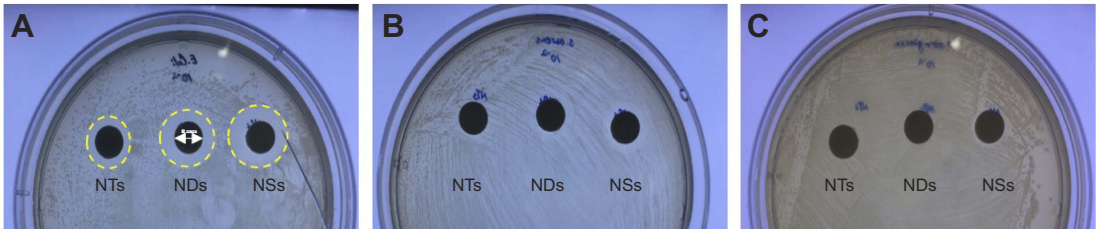


**Figure 4** Inhibition zone around Ag NPs with different shapes impregnated into paper disk: (**A**) *E. coli*, (**B**) *S. aureus*, (**C**) *P. aeruginosa*.
**Abbreviation:** Ag NPs, silver nanoparticles; NDs, disk shape; NSs, sphere shape; NTs, triangular plate shape.

inhibition region of 4.8 mm. The inhibition zones formed weakly in all Ag NPs against *S. aureus* and *P. aeruginosa* (Figure 4B and C). Therefore, the three types of Ag NPs showed a high activity against *E. coli*, and the antimicrobial activity was in the order of Ag NSs > Ag NDs > Ag NTs.

The OD growth curves were obtained in Lysogeny broth (LB) medium supplemented with different Ag NPs. The antimicrobial activity of the Ag NPs against *E. coli* could be evaluated from the growth curve. This indicates that the longer the delay in growth, the stronger the antimicrobial activity.[8,27]

From Figure 5, the Ag NSs and Ag NDs showed a higher antimicrobial activity, and their antimicrobial activity improved as the concentration of the NPs increased from 0.1 to 0.7 mg/mL. On the other hand, the Ag NTs exhibited control-like *E. coli* growth at all concentrations. Interestingly, the Ag NSs were found to be more effective in delaying the growth of *E. coli* than the Ag NDs at the same concentration.

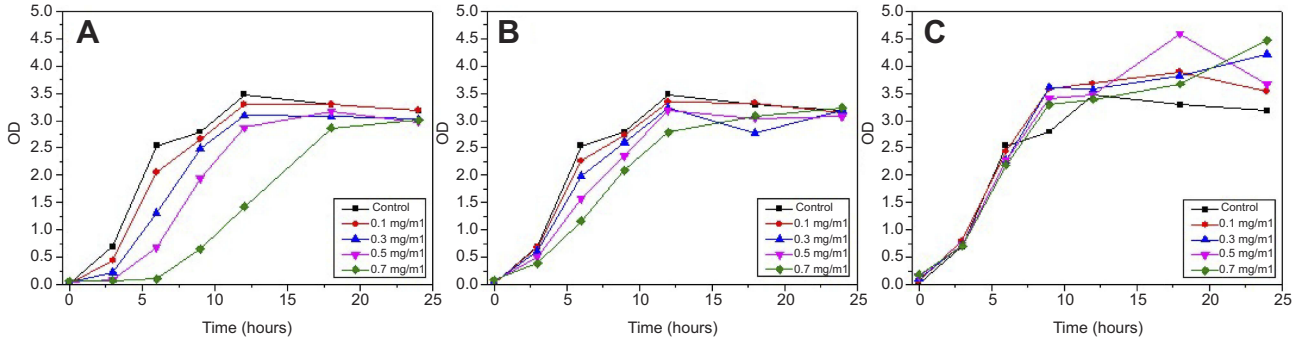


**Figure 5** OD growth curves of *E. coil* in LB broth at 37°C according to different concentrations of (**A**) Ag NSs, (**B**) Ag NDs and (**C**) Ag NTs.
**Abbreviations:** Ag NDs, disk shape; Ag NSs, sphere shape; Ag NTs, triangular plate shape.

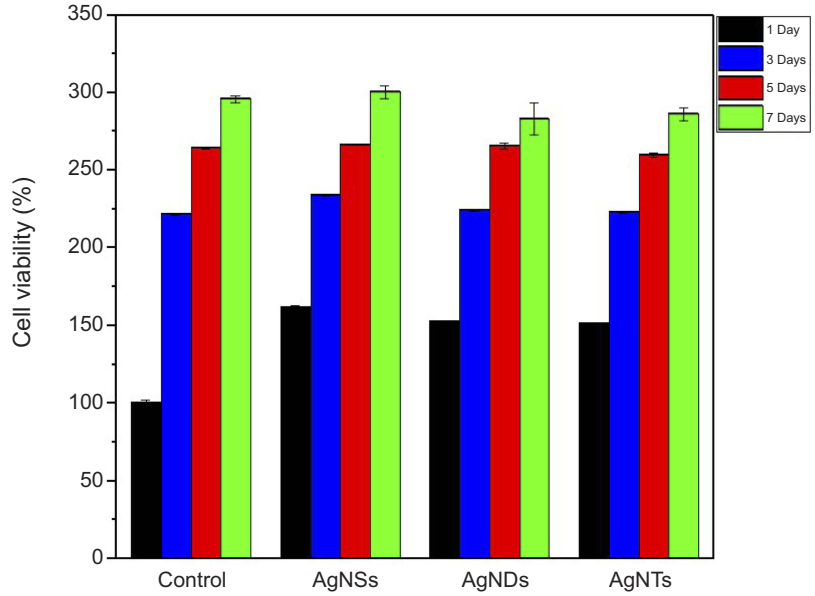


**Figure 6** Effect of the Ag NPs with different shapes on the viability of the fibroblast cells via the MTT assay.
**Abbreviations:** Ag NPs, silver nanoparticles; Ag NDs, disk shape; Ag NSs, sphere shape; Ag NTs, triangular plate shape.

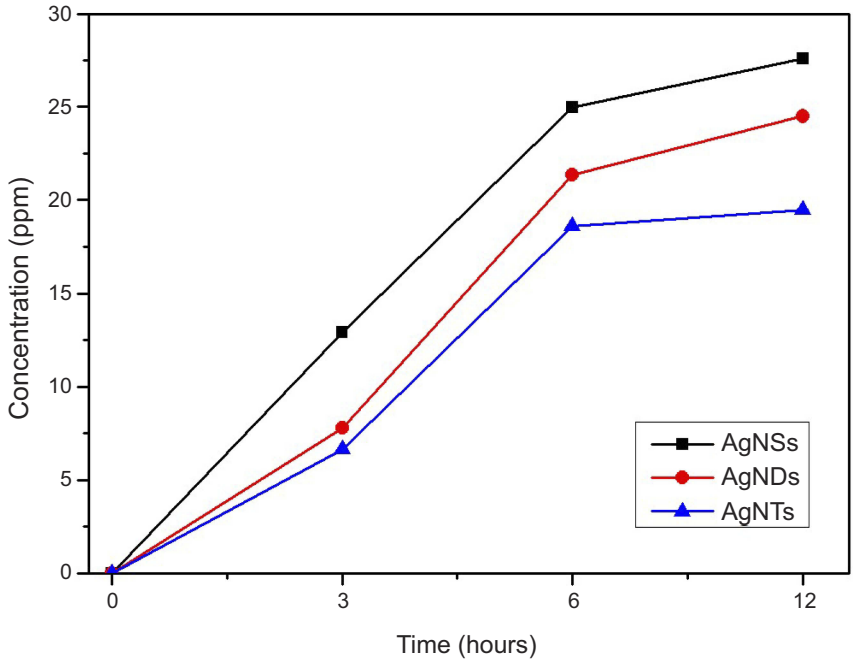


**Figure 7** Release rate of Ag ions for different Ag NPs with times.
**Abbreviations:** Ag NPs, silver nanoparticles; Ag NDs, disk shape; Ag NSs, sphere shape; Ag NTs, triangular plate shape.

That is, the Ag NSs exhibited the strongest antimicrobial activity against *E. coli*.

To confirm the applicability of the Ag NPs in the medical field, the cell viability was evaluated for one week using fibroblast cells. Figure 6 shows that the cells were well grown in all Ag NPs regardless of their shape, similar to the control group. The reason for this difference in antimicrobial activity is that the Ag NPs express a mechanism to destroy the cell membrane, leading to the death of the cell. In the case of the fibroblast cell,

however, the Ag NPs are absorbed into the cell via endocytosis.[10] This is consistent with the findings that there is no dependence on the shape of the Ag NPs.

The antimicrobial activity of the three types of Ag NPs is expected to be due to differences in the surface area depending on the morphology of the NPs. In the case of the antimicrobial activity, the Ag ions ($Ag^+$) are released from the NPs (Ag°). Therefore, the amount of Ag ions that are released is dependent on the surface area due to the shape of the NPs. When the surface area was calculated using the average particle size, the surface areas of the Ag NSs, Ag NDs and Ag NTs were 1,307±5 $cm^2$, 1,104±109 $cm^2$ and 1,028 ±35 $cm^2$, respectively. The surface area of the Ag NTs was lower than that of the Ag NSs or Ag NTs. When the release rate of the Ag ions from the Ag NPs was analyzed via ICP, the amount of Ag ions was found to have been released in the order of Ag NSs > Ag NDs > Ag NTs (Figure 7). Obviously, the antimicrobial activity of the Ag NPs was mainly dependent on their morphology, which was closely associated with the total surface area and the amount of Ag ions that were released. Therefore, the antimicrobial mechanism of Ag NPs could be explained by the penetration of Ag ions into bacterial cell for efficient killing, although the antimicrobial actions of Ag NPs are generally considered to involve various routes.

## Conclusion

Ag NPs with spherical, triangular plate and disk shapes were synthesized in an aqueous solution using a simple method. The color of the synthesized Ag NPs was visually confirmed, and the actual morphology was analyzed via TEM imaging. The TEM images indicated that the Ag NPs with different morphologies had been successfully synthesized. When the Ag NPs were evaluated using the paper disk method against *S. aureus, E. coli* and *P. aeruginosa*, they showed the highest antimicrobial activity against *E. coli*. Therefore, the OD test was performed on *E. coli* according to the concentration of the Ag NPs. As a result, a higher concentration of spherical Ag NPs was confirmed to result in a higher antibacterial activity. Therefore, the morphological dependence of the antimicrobial activity of the Ag NPs can be explained by the difference in the Ag ion release depending on the shape. Therefore, it will be possible to control the antimicrobial activity by controlling the shape and size of the Ag NPs.

## Acknowledgments

This study was financially supported by the National Research Foundation (NRF) of Korea (2018R1A2A2A05021100).

## Disclosure

The authors report no conflicts of interest in this work.

## References

1. Takeshima T, Tada Y, Sakaguchi N, Watari F, Fugetsu B. DNA/Ag nanoparticles as antibacterial agents against gram-negative bacteria. *Nanomaterials*. 2015;5:284–297. doi:10.3390/nano5010284
2. Raza M, Kanwal Z, Rauf A, Sabri A, Riaz S, Naseem S. Size- and shape-dependent antibacterial studies of silver nanoparticles synthesized by wet chemical routes. Synergistic antibacterial activity of chitosan–silver nanocomposites on *Staphylococcus aureus*. *Nanomaterials*. 2016;6:74–88. doi:10.3390/nano6040074
3. Potara M, Jakab E, Damert A, Popescu O, Canpean V, Astilean S. Synergistic antibacterial activity of chitosan-silver nanocomposites on *Staphylococcus aureus*. *Nanotechnology*. 2011;22:135101. doi:10.1088/0957-4484/22/13/135101
4. Nischala K, Rao TN, Hebalkar N. Silica–silver core–shell particles for antibacterial textile application. *Colloid Surf B*. 2011;82:203–208. doi:10.1016/j.colsurfb.2010.08.039
5. Sadeghi B, Garmaroudi FS, Hashemi M, Nezhad HR, Nasrollahi A, Ardalan S. Comparison of the anti-bacterial activity on the nanosilver shapes: nanoparticles, nanorods and nanoplates. *Adv Powder Technol*. 2012;23:22–26. doi:10.1016/j.apt.2010.11.011
6. Suresh AK, Pelletier DA, Doktycz MJ. Relating nanomaterial properties and microbial toxicity. *Nanoscale*. 2013;5:463–474. doi:10.1039/c2nr32447d
7. Kahru A, Ivask A. Mapping the dawn of nanoecotoxicological research. *Acc Chem Res*. 2013;46:823–833. doi:10.1021/ar3000212
8. Hong X, Wen J, Xiong X, Hu Y. Shape effect on the antibacterial activity of silver nanoparticles synthesized via a microwave-assisted method. *Environ Sci Pollut Res*. 2016;23:4489–4497. doi:10.1007/s11356-015-5668-z
9. Jung WK, Koo HC, Kim KW, Shin S, Kim SH, Park YH. Antibacterial activity and mechanism of action of the silver ion in *Staphylococcus aureus* and *Escherichia coli*. *Appl Environ Microbiol*. 2008;74:2171–2178. doi:10.1128/AEM.02001-07
10. Helmlinger J, Sengstock C, Groß-Heitfeld C, et al. Silver nanoparticles with different size and shape: equal cytotoxicity, but different antibacterial effects. *RSC Adv*. 2016;6:18490–18501. doi:10.1039/C5RA27836H
11. Li M, Ma Z, Zhu Y, et al. Toward a molecular understanding of the antibacterial mechanism of copper-bearing titanium alloys against Staphylococcus aureus. *AdvHealthcare Mater*. 2016;5:554–566. doi:10.1002/adma.19930050707
12. AshaRani PV, Mun GLK, Hande MP, Valiyaveettil S. Cytotoxicity and genotoxicity of silver nanoparticles in human cells. *ACS Nano*. 2009;3:279–290. doi:10.1021/nn800596w
13. Choi O, Hu ZQ. Size dependent and reactive oxygen species related nanosilver toxicity to nitrifying bacteria. *Environ Sci Technol*. 2008;42:4583–4588.
14. Hackenberg S, Scherzed A, Kessler M, et al. Silver nanoparticles: evaluation of DNA damage, toxicity and functional impairment in human mesenchymal stem cells. *Toxicol Lett*. 2011;201:27–33. doi:10.1016/j.toxlet.2010.12.001
15. Marambio-Jones C, Hoek EM. A review of the antibacterial effects of silver nanomaterials and potential implications for human health and the environment. *J Nanopart Res*. 2010;12:1531–1551. doi:10.1007/s11051-010-9900-y

16. Raza MA, Kanwal Z, Rauf A, Sabri AN, Riaz S, Naseem S. Size- and shape-dependent antibacterial studies of silver nanoparticles synthesized by wet chemical routes. *Nanomaterials*. 2016;74:1–15.
17. Alshareef A, Laird K, Cross RBM. Shape-dependent antibacterial activity of silver nanoparticles on *Escherichia coli* and *Enterococcus faecium* bacterium. *Appl Surf Sci*. 2017;424:310–315. doi:10.1016/j.apsusc.2017.03.176
18. Xia Y, Xing Y, Lim B, Skrabalak SE. Shape-controlled synthesis of metal nanocrystals: simple chemistry meets complex physics? *Angew Chem Int Ed*. 2009;48:60–103.
19. Wiley B, Sun YG, Mayers B, Xia YN. Shape-controlled synthesis of metal nanostructures: the case of silver. *Chem Eur J*. 2005;11:454–463. doi:10.1002/(ISSN)1521-3765
20. Pal S, Tak YK, Song JM. Does the antibacterial activity of silver nanoparticles depend on the shape of the nanoparticle? A study of the gram-negative bacterium *Escherichia coli*. *Appl Environ Microbiol*. 2007;73:1712–1720. doi:10.1128/AEM.02218-06
21. Cui L, Chen P, Chen S, et al. In situ study of the antibacterial activity and mechanism of action of silver nanoparticles by surface-enhanced Raman spectroscopy. *Anal Chem*. 2013;85:5436–5443. doi:10.1021/ac400245j
22. Liu W, Wu Y, Wang C, et al. Impact of silver nanoparticles on human cells effect of particle size. *Nanotoxicology*. 2010;4:319–330. doi:10.3109/17435390.2010.483745
23. Park MV, Neigh AM, Vermeulen JP, et al. The effect of particle size on the cytotoxicity, inflammation, developmental toxicity and genotoxicity of silver nanoparticles. *Biomaterials*. 2011;32:9810–9817. doi:10.1016/j.biomaterials.2011.08.085
24. Gao MJ, Sun L, Wang ZQ, Zhao YB. Controlled synthesis of Ag nanoparticles with different morphologies and their antibacterial properties. *Mat Sci Eng C*. 2013;33:397–404. doi:10.1016/j.msec.2012.09.005
25. Parnklang T, Lertvachirapaiboon C, Pienpinijtham P, Wongravee K, Thammacharoena C, Ekgasit S. $H_2O_2$-triggered shape transformation of silver nanospheres to nanoprisms with controllable longitudinal LSPR wavelengths. *RSC Adv*. 2013;3:12886–12894. doi:10.1039/c3ra41486h
26. Cheon JY, Park WH. Green synthesis of silver nanoparticles stabilized with mussel-inspired protein and colorimetric sensing of lead(II) and copper(II) ions. *Int J Mol Sci*. 2016;17:2006. doi:10.3390/ijms17122006
27. Sui M, Zhang L, Sheng L, Huang S, She L. Synthesis of ZnO coated multi-walled carbon nanotubes and their antibacterial activities. *Sci Total Environ*. 2013;452:148–154. doi:10.1016/j.scitotenv.2013.02.056